

NASA TECHNICAL
MEMORANDUM



NASA TM X-725

NASA TM X-725

CASE FILE
COPY

VISUAL STUDY OF SWIRLING
AND NONSWIRLING TWO-PHASE
TWO-COMPONENT FLOW
AT 1 AND 0 GRAVITY

by David G. Evans;
Lewis Research Center,
Cleveland, Ohio

TECHNICAL MEMORANDUM X-725

VISUAL STUDY OF SWIRLING AND NONSWIRLING TWO-PHASE
TWO-COMPONENT FLOW AT 1 AND 0 GRAVITY

By David G. Evans

Lewis Research Center
Cleveland, Ohio

NATIONAL AERONAUTICS AND SPACE ADMINISTRATION

NATIONAL AERONAUTICS AND SPACE ADMINISTRATION

TECHNICAL MEMORANDUM X-725

VISUAL STUDY OF SWIRLING AND NONSWIRLING TWO-PHASE

TWO-COMPONENT FLOW AT 1 AND 0 GRAVITY

By David G. Evans

SUMMARY

Flow visualization tests were made of various swirling and nonswirling two-phase two-component flow regimes at 1 and 0 g in a 1/2-inch-diameter clear plastic tube. Air and water at adiabatic-isothermal conditions were used as the two components. Bubbly- and slug-flow regimes were investigated. Swirling flow was generated by using coiled wires with diameters-per-twist ratios (pitch length between wire coils or ribbon twists expressed in tube diameters) of 3.1, 4.4, and 8.5 and twisted ribbons with corresponding ratios of 2.7, 4.2, and 7.5.

An analysis was made of high-speed motion pictures taken of the various flow regimes. The results of the analysis, presented in the form of flow models, indicated that gravity had an effect on the phase orientation and turbulence level of the flow. Generally, under conditions of 0 g, bubble turbulence became less, and the dispersion of bubbles became more homogeneous across the tube and tube wall boundary layer than at 1 g. The notable difference between swirling and nonswirling flow was the formation of distinct cores of bubbles with swirling flow. Vertical swirling flow at 1 g with coiled wires closely resembled flow at 0 g.

The use of a zero-gravity aircraft facility with the experimental package either restrained or allowed to float freely inside the aircraft to achieve weightlessness gave satisfactory and repeatable results. The relatively short periods of weightlessness and the degree of variation from perfect weightlessness inherent in this type of facility did not affect the results of the investigation.

INTRODUCTION

Considerable work has been done in the areas of flow visualization, heat transfer, and pressure loss with fluid regimes involving the simultaneous flow of liquids and vapors (two-phase flow). References 1 to 4 are noted as examples. These investigations have been carried out in an environment of gravity where the vapor phase was acted upon by the buoyant force of the liquid. Buoyancy, or in other words the effect of gravity, was frequently a major factor contributing to the visual appearance, heat transfer, pressure loss, or other characteristics unique to the conditions of the flow regimes investigated.

With the advent of operations in space, various types of fluid systems involving two-phase flow will be required for space vehicle cooling, life support, power generation, propulsion, and other uses. The operation of these systems in space will reduce the normal environment of 1 g to one of zero or near-zero g, in which a vapor would exhibit no buoyancy when dispersed in a liquid.

Generally, the heat-transfer and pressure-loss characteristics of two-phase flow are functions of many factors, such as velocity, turbulence, stability, density, orientation, etc. of each phase. (Terminology is defined in appendix A.) The degree to which gravity affects these individual factors will determine the net effect it has on the heat transfer and pressure loss. Furthermore, the size, weight, efficiency, and operational stability of the entire fluid system and the degree to which weightless operation in space affects them will depend on these characteristics.

Several experimental investigations have therefore been undertaken at the Lewis Research Center to determine the effects of weightlessness on two-phase flow (e.g., refs. 5 and 6). The present investigation was undertaken to study the effects of weightlessness on two-phase flow orientation and turbulence. The results of the investigation are presented in the form of photographic comparisons made between the various two-phase flow regimes investigated at 1 and 0 g. All tests were carried out within a 1/2-inch-inside-diameter clear plastic tube either with or without coiled wire or twisted-ribbon swirl inserts. The use of swirl generators as an aid to heat transfer has been investigated by many others (e.g., refs. 7 to 9). Because these devices may prove useful in space applications, they were included.

Since the intent of the investigation was to observe the effects of weightlessness on simple two-phase regimes, the many additional factors such as heat transfer were left to later, more detailed investigations. The two phases were generated by injecting air into water (city tap water) flowing through the 1/2-inch tube. Bubbly- and slug-flow regimes were generated.

The weightless portions of the investigation were carried out in two specially modified aircraft capable of flying weightless trajectory maneuvers for periods up to 15 seconds. Two test procedures were evaluated: restraining and free floating the experimental package in the aircraft. This evaluation was made to determine whether the less risky and less complicated method of restraining the package caused any apparent differences in the behavior of the flow regimes. The use of the aircraft facilities, in general, for this type of fluid experimentation was also evaluated.

A narrated 16-millimeter motion-picture supplement C-225 has been prepared and is available on loan. A request card and a description of the film are included at the back of this report.

DESCRIPTION OF APPARATUS

The 1/2-inch-inside-diameter clear plastic test section and the various coiled-wire and twisted-ribbon swirl generators used in the investigation are shown in figure 1. The test section was 18 inches long, optically clear, and

provided with a scale graduated in increments of 0.1 inch. The three coiled-wire swirl generators were 1/8-inch wire, coiled to diameters-per-twist ratios (pitch length between coils or ribbon twists expressed in tube diameters) of 3.1, 4.4, and 8.5. The three twisted ribbons were made of 1/16-inch clear plastic, twisted to diameters-per-twist ratios of 2.7, 4.2, and 7.5. The generators, when used, were inserted inside the test section and keyed to prevent rotation. Clearances between the generators and the inside of the tube wall varied from 0 to 1/32 inch.

Two-phase flow was generated in the following manner, as shown in the flow diagram of the experimental apparatus (fig. 2(a)): Pressurized air was supplied from a small aircraft pressure-vacuum vane-type air pump to a surge tank. It was bled through the pressure regulator A to the balloon expulsion bladder B located in the expulsion tank C filled with city tap water. As the balloon inflated, water was forced to flow from the expulsion tank through the test section to the collection tank D. Additional air was bled from the surge tank, regulated through E, and injected just upstream of the test section through a fine-mesh screen, which generated two-phase flow. A second collection tank G, consisting of a balloon collector in a vented tank, collected the flow during intervals of weightlessness. Otherwise, water, which periodically blocked the air vent F on collection tank D during weightlessness, would have caused unsteady flow. After each run, the contents of the balloon collector were forced out with pressurized air, along with the contents of collection tank D, back through the test section to the expulsion tank.

Flow velocities in the test section were controlled by restricting the flow of displaced air through the collection tank vents F and H. Air-to-water ratios were controlled by adjusting regulators A and E. Flow pressures entering the test section were held constant at 2 pounds per square inch above ambient pressure by the pressure regulator located on the surge tank, which resulted in a variation in inlet pressure of from 17 to 9 pounds per square inch absolute between sea level and maximum altitude conditions covered during the investigation.

Bubble size also decreased during the course of the investigation because of a gradual clogging of the air injection screen. Initially, bubble diameters averaged between 0.05 and 0.10 inch but later diminished to between 0.01 and 0.03 inch. Bubble size therefore became an independent variable, which required that many of the tests be repeated.

A high-speed 16-millimeter motion-picture camera with a 60-cycle timing light, photographing a 23° field of view, was located opposite the test section 12 inches downstream of the air injector. The camera was mounted perpendicular to, and at a 45° angle below, the test section (as shown in fig. 2(b)), with the inch scale and an events counter mounted as shown.

All operational functions on the experimental package were performed remotely to facilitate free floating of the package inside the aircraft. The electric power, control, and instrumentation leads were brought to the package from a control box through a flexible 20-foot cable. The experimental package and control box are shown in figure 3. Camera speeds were controlled by a variable transformer shown in the photograph.

PROCEDURE

A total of 65 tests were made, during which two-phase flow regimes were generated in the manner noted in the preceding section. The tests covered a range of bubble velocities from 1 to 3 feet per second, air-to-water ratios from approximately 1/2 to 80 percent by volume, nonswirling flow and swirling flow generated with the use of the three coiled-wire and three twisted-ribbon inserts, horizontal and vertical flow at 1 g, and flow at 0 g in which the restrained and the free-floating techniques of handling the experimental package were used.

Bubble velocities and air-to-water ratios were measured from the high-speed motion pictures taken during each test. The inch scale and the time trace appearing on the film were used to measure the time required for the bubbles to travel 1 inch. Average bubble velocities were measured. The number and the diameter of bubbles observed in the flow per inch of tube length were used to compute the ratio of the volume of air to the volume of water. In flow regimes where the bubbles were tightly packed, the total number and the average diameter of the bubbles were estimated.

Periods of near-zero g suitable for conducting the weightless portions of the experiment were obtained in specially modified aircraft flying through a portion of a ballistic path, as noted previously. Details of the aircraft maneuver are in appendix B.

Initial 0-g flights were made in an Air Force C-131b type aircraft, in which the relatively large interior dimensions permitted free floating of the experimental package during weightlessness, which eliminated the transmission of random accelerations of the aircraft to the package. These random accelerations were caused by maneuvering corrections, manual control deficiencies, and air turbulence encountered during the maneuver and averaged approximately ± 0.02 g in magnitude. Such accelerations usually resulted in contact between the fuselage and the free-floating package before the duration of weightlessness was completed, which disrupted the experiment for the remainder of the trajectory. The flow regimes within the test section, however, usually stabilized to their 0-g configuration, and the motion pictures were taken before contact. Figure 4(a) shows the package floating freely in the C-131b aircraft during one of these maneuvers.

Several weightless trajectories were also flown with the package restrained (strapped) to the floor of the C-131b aircraft. Insulation was used to eliminate transmission of engine vibration to the package. The package and associated equipment restrained in position in the C-131b aircraft are shown in figure 4(b). The balance of the investigation was completed in the AJ-2 aircraft when it became available, with the package strapped to the aircraft through insulation.

RESULTS AND DISCUSSION

The photographic observations that were made of the various two-phase flow regimes photographed at 1 and 0 g are discussed in detail. Short segments of the 16-millimeter film are included in the film supplement. Representative photographic enlargements from the films are presented in tables I to III with the flow going from left to right. Schematic flow models are also presented in the

tables, which show in cross section the various orientations of the two phases as interpreted from the films. The comparisons and results, however, can be more clearly observed in the film supplement.

The observations made at 1 g are similar to those that have been established by others. They are presented herein, however, as an aid in making comparisons with the flow regimes at 0 g.

Nonswirling Flow

In test runs 2 to 6, 36 to 40, and 52 to 55 no swirling devices were used (see table I). Tests at 1 g were made of horizontal and vertically upward and downward flow. Tests at 0 g were made in the restrained position aboard the AJ-2 aircraft.

Horizontal flow at 1 g. - The bubbles were oriented predominantly in the upper half of the tube during horizontal flow at 1 g as was expected, since gravity was the predominant force at the bubble velocities and percentages of air volumes investigated (table I(a)). The bubbles in contact with the tube wall remained on the wall and traveled at velocities somewhat lower than those one or two rows radially inward from the wall. The radial gradient in velocity indicated that bubbles were located in both the wall boundary layer and the free stream, which caused some overriding and turbulence at the interface between the high- and the low-velocity rows of bubbles.

In run 4 the smaller bubbles injected were oriented toward the top of the tube along the tube wall, whereas the larger bubbles were oriented in the free stream toward the center of the tube. In run 5, some bubbles coalesced and frequently formed large bubbles (0.30-in. diam.), which remained buried in the pack.

Reynolds numbers in the liquid phase, as defined in appendix A, were above the critical and the transitional values normally associated with single-phase pipe flow (table I), that is, a critical value of approximately 2000 and a transitional region between values of 2000 and 3000.

In run 54 the size of the bubbles injected was considerably smaller than those in runs 4 and 5. Even though the percentage of air volume was low, the bubbles were distributed across more of the tube than in runs 4 and 5. A high gradient in bubble velocity existed across the free-stream boundary-layer interface. The kinetic, turbulent, and viscous forces acting on the bubbles appeared more noticeable than in runs 4 and 5, as might be expected since the buoyant forces (bubble volume) decreased more rapidly than the viscous forces (bubble surface area) with decreasing bubble diameter.

Vertical flow at 1 g. - The dispersion of bubbles during vertical flow at 1 g became nearly uniform across the free stream and the outer extremity of the wall boundary layer (tables I(b) and (c)). Generally, few or no bubbles were observed on the tube wall. In the early runs, in which the average bubble diameter was 0.08 inch, some turbulence was observed, which appeared to be due to the buoyant force that drove the bubbles upward through the liquid at velocities

higher than free-stream liquid velocities. This turbulent motion occasionally drove the bubbles toward the tube boundary layer, where they rebounded and returned to the free stream. The tube wall remained all liquid. As bubble size was diminished, however, bubble turbulence diminished, and a marked increase in the bubble velocity gradient was observed. This increase indicated that the bubbles were penetrating the boundary layer and remaining there. Flow vertically downward (run 55) appeared similar to flow vertically upward (run 52) except for a reduction in the bubble velocity gradient.

Flow at 0 g. - The bubbles during flow at 0 g generally became more equally dispersed across the free-stream portion of the tube and were more prevalent in the boundary layer and on the tube wall than at 1 g. Also, less bubble turbulence was observed in the free stream, the boundary layer, and the interface between them than at 1 g, even though Reynolds numbers were above the critical number. Some turbulence was observed, however, in the runs in which bubbles or slugs and bubbles of widely varying size were flowing in close proximity. Such conditions prevailed when the bubbles coalesced or when the volume of air injected was such as to produce slugs, as in run 40. Pockets of smaller bubbles gathered among the slugs and occasionally in the low-velocity liquid layer surrounding the slugs. In runs 36b and 38, in which the bubbles coalesced, the large bubbles resulting from coalescence moved to the center of the free stream and remained within an annular dispersion of smaller bubbles, just as noted for horizontal flow at 1 g (run 4).

Swirling Flow with Coiled Wires

The three coiled-wire swirl generators were tested in runs 1a to 1d, 7 to 14, 29 to 35, and 41 to 50 (see table II). Tests at 0 g were made from the restrained and the free-floating positions aboard the C-131b aircraft and in the restrained position aboard the AJ-2 aircraft. During the runs aboard the C-131b aircraft the two techniques of handling the experimental package during weightlessness were evaluated on the basis of comparing bubble coalescence, turbulence, and phase orientation.

Reynolds numbers for all runs in which bubble velocities were measured were above the critical and transitional values normally associated with single-phase pipe flow (see table II). The magnitude of the induced buoyant force caused by swirling the flow is also given in table II. The term is referred to herein as the "induced radial acceleration" and is defined in appendix A; the term is in units of gravity.

Horizontal flow at 1 g. - The predominant difference between swirling and nonswirling horizontal flow at 1 g was the reorientation of the bubbles into a distinct core, as shown by the flow models in table II(a). The rate at which the core rotated about its center axis varied with the coil ratio of the wires in all but one run, run 56. In that run, the bubbles were smaller and air volume was lower than in the other runs, and a tightly packed froth-type flow regime extended over most of the free-stream and boundary-layer portions of the tube. The froth appeared to create a viscous resistance to rotation and a high wall-velocity gradient. In the other runs, the wire inserts did not impart sufficient core rotation to prevent the core from entering the upper half of the tube and

the wall boundary layer between wires. In this case, turbulence was generated around the wires at the points where they crossed over the top of the tube. In run 41, however, the entire core was deflected intact to the side of the tube approximately opposite the wire, followed a corkscrew path through the tube, and showed very little effects of gravity.

Bubble penetration of the boundary layer was found to be a function of bubble diameter, core diameter, and the magnitude of the induced radial force for the conditions involved. Penetration, as noted by the intensity of the wall bubble velocity gradient, increased with increasing core diameter and decreasing bubble diameter and radial force. Free-stream turbulence, as in the case of nonswirling flow, was higher in the flow regimes with the largest variations in bubble size, such as in run 35. This run was also the only one in which bubble coalescence was observed. Relatively large bubbles were observed in runs 7 and 50, but no coalescence took place in the plane of the camera.

Vertical flow at 1 g. - The formation and rate of rotation of the bubble cores during vertical flow at 1 g were not so distinct as noted previously for horizontal swirling flow. Dispersion of the bubbles was nearly uniform across the tube for the wire with a diameters-per-twist ratio of 8.5, as had generally been the case for nonswirling vertical flow at 1 g (see tables II(b) and (c)).

Turbulence, in general, was slight and was confined to those runs where the bubbles were contacting the wire, such as runs 33, 34, and 57, or where large bubbles were present, such as run 34. No coalescence was observed among the small bubbles in run 34; however, they completely masked the larger bubbles located toward the center of the tube, where coalescence may have taken place. No indication of coalescence was observed in any other runs. Vertically downward flow in run 58 appeared similar to upward flow in run 59 except for a more perceptible deflection and corkscrewing of the core in its attempt to miss the wire.

Flow at 0 g. - No significant differences were found between the appearance of the vertical flow at 1 g and the weightless flow regimes at 0 g (see table II(d)). A few more instances of bubble coalescence or possible coalescence were present at 0 g than in vertical flow at 1 g.

Two additional items to note in table II(d) were (1) the achievement of comparable flow regimes between the restrained and the free-floating methods (runs 8 and 11, as well as other runs) and (2) the generation of a slug-flow regime in runs 31 and 32. In regard to the first item, the lack of any noticeable difference in the flow regimes between the free-floating and the restrained methods indicated that the less risky and less complicated method of restraining the experimental package to the aircraft was satisfactory. Approximately one of every three weightless runs with the experimental package in the restrained position was unusable because of excessive buffeting of the aircraft or pilot control difficulties encountered during the maneuver. Approximately the same ratio of free-floating runs was terminated, however, because of contact of the experimental package with the fuselage before the flow regime could assume its 0-g configuration or before the high-speed motion pictures could be taken.

In regard to the second item, run 31 consisted of slugs averaging $1/2$ inch in length intermixed with bubbles ranging from 0.05 to 0.40 inch in diameter. Considerably more bubble turbulence and bubble distortion were observed than in any of the other flow regimes investigated. The air remained in a well-defined core that rotated at almost the same rate as the corresponding all-bubble flow regimes. When the air volume was increased 10 percent to approximately 65 percent (run 32), the flow consisted almost entirely of slugs averaging 2 inches in length. The slugs remained centered in the tube; however, the wire imparted no noticeable rotation to the flow. Considerable wave motion in the liquid film surrounding the slugs was observed near the ends of the slugs.

Swirling Flow with Twisted Ribbons

The three twisted-ribbon swirl generators were tested in runs 15 to 28 and 51 at 0 g (table III). The experimental package was tested in both the restrained and the free-floating positions. No comparative tests were made at 1 g. Because of the relatively well guided and confined shape of the flow channels formed by the twisted-ribbon inserts compared with the nonswirling and the coiled-wire configurations, it was felt that no significant difference would exist between the various 1- and 0-g flow regimes. A comparison, however, between the twisted-ribbon and the coiled-wire techniques of swirling and separating the flow at 0 g was desired, as well as the additional comparisons that could be made between the restrained and the free-floating techniques.

Flow at 0 g. - The flow regimes at 0 g were characterized as being less turbulent with a greater tendency toward bubble coalescence than all other flow regimes investigated at 1 or 0 g. Some turbulence, however, was observed locally around coalescing sites. A greater tendency to coalesce was observed with the more tightly twisted ribbons. Some turbulence was also observed in the free stream for the runs with the ribbons of a diameters-per twist ratio of 2.7 because of the severity of the corkscrew path presented by the tightly twisted ribbon. The diameter term required for computing Reynolds numbers was approximated at four-fifths of the tube diameter. The resulting Reynolds numbers were higher than the critical and transitional values.

The twisted-ribbon flow regimes were also characterized by the formation of two bubble cores, one on either side of the ribbon, that did not enter the tube wall or the ribbon wall boundary layer. No gradients in bubble velocity were perceptible across the cores or at the outer extremities of the cores. Tube and ribbon walls therefore appeared to be all liquid.

The only other noticeable effect that variations in the diameters-per-twist ratio had on the appearance of the flow regimes, other than on the turbulence level, was on the bubble density, and hence on the size of the cores. The cores, in general, were more loosely packed for the ribbon with a diameters-per-twist ratio of 7.5 than for the more tightly packed cores of the ribbons with ratios of 4.2 and 2.7.

Comparable flow regimes were obtained between runs 16 and 18, 17 and 19, 21 and 22, and 26 and 27, which were used as comparison checks between the free-floating and the restrained methods. These comparison checks, as previously

noted, were satisfactory. Runs 16 and 18, as well as runs 21 and 22, indicated no tendency toward bubble coalescence. Runs 17 and 19 and runs 26 and 27 coalesced, and, in addition, runs 26 and 27 both developed the same slug-bubble-flow regimes. It was therefore concluded, just as for coiled wires, that the restrained method of conducting the experiment in the aircraft was satisfactory for swirling flow.

SUMMARY OF RESULTS

Flow visualization tests were made of various swirling and nonswirling two-phase, two-component flow regimes at 1 and 0 g in a 1/2-inch-diameter tube. Air and water at isothermal-adiabatic conditions were used as the two components. The following is a summary of the observations that were made over the range of variables and conditions stipulated for the experiment:

Nonswirling flow at 1 g. - In horizontal nonswirling flow at 1 g, bubble turbulence was generated in the area between the free stream and the boundary layer because of an overriding of bubbles traveling at dissimilar velocities. Also, some coalescence occurred among the larger bubbles injected, which resulted in bubble growths up to 0.30 inch in diameter. As the size of the bubbles injected was reduced, bubble dispersion became slightly more uniform across the free stream.

In vertically upward flow, bubble turbulence in the free stream decreased, but the velocity gradient and bubble penetration of the boundary layer increased with increasing air volumes from 10 to 55 percent or with decreasing bubble diameters from 0.08 to 0.03 inch in diameter. The appearance of flow vertically downward resembled vertically upward flow except for a slight reduction in the bubble velocity gradient.

Nonswirling flow at 0 g. - In bubbly nonswirling flow regimes, less turbulence and a more even distribution of bubbles were present at 0 g than for either vertical or horizontal flow at 1 g. Generally, higher gradients in bubble velocity were observed at 0 g, which indicated greater bubble penetration of the wall boundary layer. In slug- or bubbly-flow regimes where large variations in bubble size were present, bubble turbulence was observed, with the small bubbles located in an annular position around a center core of large bubbles.

Swirling flow with coiled wires at 1 g. - In horizontal swirling flow with coiled wires at 1 g, distinct rotating cores of bubbles were formed. The rate of rotation and bubble density within these cores varied with the coil ratio of the wires and with the degree to which the bubbles penetrated the tube wall boundary layer. Bubble penetration of the boundary layer increased with increasing core diameters and decreasing bubble diameter. The rate of rotation, however, was not sufficient to prevent the cores from deflecting toward the top of the tube and entering the wall boundary layer between wires, which generated considerable turbulence. Free-stream turbulence occurred in flow regimes with large variations in bubble size.

In vertical flow, the formation and the rate of rotation of the bubble cores were not so perceptible as in the comparable horizontal swirling flow regimes.

The cores were larger in diameter and of lower bubble density. Bubble dispersion was nearly uniform across the free stream and outer extremity of the wall boundary layer. Bubble turbulence occurred around the wires when core diameters exceeded the inside envelope diameter of the wires because the pitch of the coils exceeded the rate of core rotation. Vertically downward flow appeared similar to vertically upward flow except for a perceptible corkscrew motion of the core in its attempt to miss the wire.

Swirling flow with coiled wires at 0 g. - The bubbly-flow regimes at 0 g resembled the vertical flow regimes at 1 g except for the appearance of a moderate amount of bubble coalescence. One combination slug-bubble-flow regime exhibited a considerable amount of flow turbulence. By comparison, one all-slug-flow regime that had approximately 10 percent more air exhibited no core rotation and relatively little turbulence. In general, similar flow regimes were obtained whether the experimental package was restrained to the airplane or allowed to float freely during the periods of weightlessness.

Swirling flow with twisted ribbons at 0 g. - Two distinct cores of bubbles were formed in swirling flow with twisted ribbons at 0 g that were less turbulent and more coalescent in nature than all other flow regimes investigated at 1 or 0 g. Some bubble turbulence was observed around coalescence sites for all ribbons tested and along the corkscrew path created by the tight twist of the ribbon with a diameters-per-twist ratio of 2.7. No bubbles were observed in either the tube or the ribbon wall boundary layers. Comparable flow regimes including coalescence and slug formation tendencies were obtained whether the experimental package was free floated or restrained to the aircraft.

CONCLUDING REMARKS

Gravity, bubble diameter, and the percentage of air present had an effect on the orientation and the turbulence level of both phases over the range of test variables and conditions incurred in both nonswirling and swirling flow. Less bubble turbulence was observed generally at 0 g than at 1 g. Greater bubble dispersion across the free stream for swirling flow and greater bubble penetration of the tube boundary layer for nonswirling flow were observed at 0 g than at 1 g. Because these effects of gravity were most noticeable in the area of the tube boundary layer, it would be expected that the pressure-loss and heat-transfer characteristics would also be affected. Further work, however, is required in these areas to determine what the effects are.

In nonswirling flow, regardless of tube orientation or gravity, bubble coalescence always occurred above an air volume of 60 percent and never occurred below a volume of 30 percent. In swirling flow with coiled wires, bubble coalescence always occurred above an air volume of 25 percent and never occurred below a volume of 10 percent. With twisted ribbons, coalescence occurred over the entire range of air volumes covered (1 to 36 percent). No conclusions could be drawn as to the effect of bubble size or flow turbulence on coalescence.

The use of the zero-gravity aircraft facility with the experimental equipment either restrained or free floated inside the aircraft gave satisfactory and

repeatable results for the swirling flow regimes investigated. No comparative tests on nonswirling flow were made. The relatively short durations of weightlessness (5 to 15 sec) and the degree of variation from 0 g during the weightless periods (± 0.02 g) did not affect the result.

Lewis Research Center
National Aeronautics and Space Administration
Cleveland, Ohio, May 9, 1963

APPENDIX A

DEFINITION OF TERMS

Air-to-water ratio	ratio of measured volumes of air and water present in test section, percent; also referred to as "percentage of air volume" or "air volume"
Diameters-per-twist (or coil) ratio	pitch length between ribbon twists or wire coils expressed in tube diameters (see fig. 1)
Flow regime	configuration assumed by fluid as dictated by environment and conditions under which it is flowing in tube
Induced radial acceleration	<p>buoyant force acting radially inward around periphery of swirling vapor core, induced by rotation of core, divided by 32.17 ft/sec²;</p> <p>Induced radial acceleration</p> $= \frac{(\text{Tangential velocity at periphery of core})^2}{\text{Core radius} \times 32.17}$
Phase	portion of fluid that is liquid (liquid phase) or vapor (vapor phase)
Phase orientation	relative position of liquid and vapor phases within flow regime
Reynolds number	<p>computed by using kinematic viscosity of water μ/ρ (where μ and ρ are viscosity and density coefficients at 75° F, respectively), average bubble velocity, and inside diameter of the tube (four-fifths of inside diameter was used as approximation for twisted-ribbon runs):</p> $\text{Reynolds number} = \frac{\text{Bubble velocity} \times \text{tube diameter}}{\left(\frac{\mu}{\rho}\right)_{\text{H}_2\text{O}} \times 32.17}$
Turbulence	nonuniform, random, or irregular motion of either or both phases of the flow; note that all but one of the flow regimes were turbulent as defined by Reynolds number; however, the term was not used in this sense

APPENDIX B

ZERO-GRAVITY FLIGHT MANEUVER

The 0-g portion of the experiment was carried out in two aircraft specially modified for flying the 0-g maneuver: an Air Force C-131b and an NASA AJ-2 (fig. 5). The 0-g maneuver (fig. 6) was initiated by accelerating the aircraft in a shallow dive, which was followed by a $2\frac{1}{2}$ -g pullup to a 30° to 40° climb.


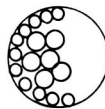
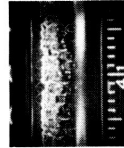
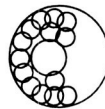
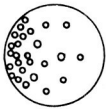
At this point, aircraft power was reduced and the plane was manually controlled to maintain a condition of zero acceleration along its three axes. This control resulted in the aircraft's following a portion of a ballistic path, during which time the aircraft and the experimental package were weightless. The duration of the weightless period was limited by the speed, the controllability, and to a lesser extent the structural characteristics of the aircraft and the skill and level of experience of the pilot. The duration of this period varied between 5 and 15 seconds. Weightlessness was terminated by a $2\frac{1}{2}$ -g pullout maneuver to straight and level flight. Additional comments and photographs are included in the film supplement to this report and in a narrated 16-millimeter motion picture entitled "Zero-Gravity Flight Facility" (Lewis Film C-217).

REFERENCES


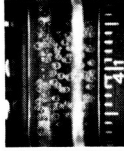
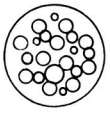
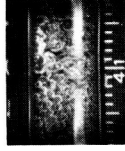
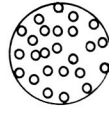
1. Martinelli, R. C., et al.: Isothermal Pressure Drop for Two-Phase, Two-Component Flow in a Horizontal Pipe. ASME Trans., vol. 66, no. 2, Feb. 1944, pp. 139-151.
2. Hsu, Yih Yun, and Graham, Robert W.: A Visual Study of Two-Phase Flow in a Vertical Tube with Heat Addition. NASA TN D-1564, 1963.
3. Griffith, Peter, and Wallis, Graham B.: Two-Phase Slug Flow. Paper 60-HT-28, ASME, 1960.
4. Wallis, Graham B., and Griffith, Peter: Liquid and Gas Distributions in a Two-Phase Boiling Analogy. Tech. Rep. 13, M.I.T., Dec. 1958.
5. Papell, S. Stephen: An Instability Effect on Two-Phase Heat Transfer for Subcooled Water Flowing Under Conditions of Zero Gravity. Paper 2548-62, Am. Rocket Soc., Inc., 1962.
6. Usiskin, C. M., and Siegel, R.: An Experimental Study of Boiling in Reduced and Zero Gravity Fields. Weightlessness - Physical Phenomena and Biological Effects, Elliot T. Benedikt, ed., Plenum Press, 1961, pp. 75-96. (See also Jour. Heat Transfer (ASME Trans.), ser. C, vol. 83, no. 3, Aug. 1961, pp. 243-253.)
7. Kreith, F., and Margolis, D.: Heat Transfer and Friction in Swirling Turbulent Flow. 1958 Heat Transfer and Fluid Mech. Inst., Stanford Univ. Press, pp. 127-134.
8. Gambill, W. R., and Greene, N. D.: A Preliminary Study of Boiling Burnout Heat Fluxes for Water in Vortex Flow. Preprint 29, AIChE, 1958.
9. Gambill, W. R., Bundy, R. D., and Wansbrough, R. W.: Heat Transfer, Burnout, and Pressure Drop for Water in Swirl Flow Through Tubes with Internally Twisted Tapes. Preprint 22, AIChE, 1960.

TABLE I. - NONSWIRLING TWO-PHASE FLOW

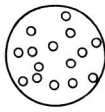
(a) Horizontal flow at 1 g

Run	Approximate air volume, percent	Reynolds number	Flow model		Average velocity, ft/sec	Bubble					
			Full-scale cross section	Reduced side view (Flow )		Diameter, in.		Coa- les- cence	Velocity gradient	Turbulence	
						Average	Range			Wall	Free stream
4	34	5,650			1.4	0.10	0.06 - 0.19	No	Slight	None	Slight
a ₅	29	11,700		-----	2.9	.09	.06 - .30	Yes	Slight	Slight	Moderate
54	1	-----		-----	---	.02	.01 - .03	No	High	None	Slight

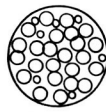
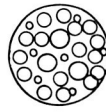

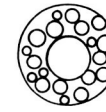
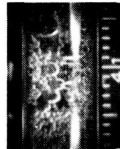
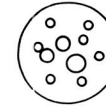
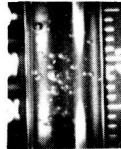
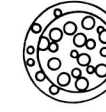
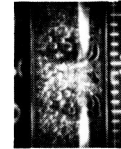
(b) Vertically upward flow at 1 g

2	6	5,250		-----	1.3	0.08	0.04 - 0.10	Slight	No bubbles	Moderate
3	6	6,450	Same as run 2		1.6	.08	.04 - .10	Slight	No bubbles	Moderate
a ₆	18	13,700			3.4	.09	.04 - .12	Moderate	None	Slight
52	4	-----		-----	---	.03	None	High	None	None

(c) Vertically downward flow at 1 g

55	3	-----		-----	---	0.03	None	No	Slight	None	None
----	---	-------	---	-------	-----	------	------	----	--------	------	------


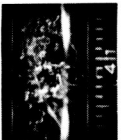
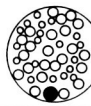

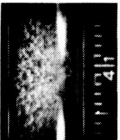



(d) Flow at 0 g (experimental package restrained)

a36a	37	5,650		-----	1.4	0.07	0.03 - 0.07	No	High	None	None
36b	47	5,650		-----	1.4	.07	.03 - .13	Yes	Moderate	Slight	Moderate
37	42	6,050		-----	1.5	.07	.02 - .13	Pos- sibly	High	Slight	Moderate
38	55	8,470			2.1	.12	.03 - .40	Yes	Moderate	None	Slight
39	1	5,650			1.4	.05	.03 - .14	No	Moderate	No bub- bles	None
40	75	8,470			2.1	.08 and slugs 0.40 by 0.50 in. long	.03 - .50	Yes	Moderate	Slight	None


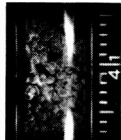

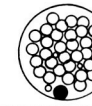
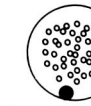
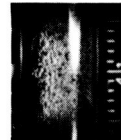
^aIncluded in film supplement.

TABLE II. - SWIRLING TWO-PHASE FLOW WITH COILED-WIRE SWIRL GENERATORS

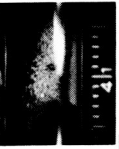
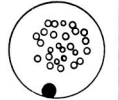
(a) Horizontal flow at 1 g

Run	Insert diameters- per-coil ratio	Experi- mental technique	Approximate air volume, percent	Approximate core diameter, in.	Approximate core rotation, diam/rev- olution	Induced radial acceler- ation, g	Reynolds number	Flow model		Bubble							
								Full-scale cross section	Reduced side view (Flow ↑)	Average velocity, ft/sec	Diameter, in. Average	Range	Coales- cence	Velocity gradient	Turbulence		
															Wall	Free stream	
35	8.5	-----	84	0.45	12	0.4	8,060			2.0	0.2	0.05 - 0.50	Yes	Slight	Mod- erate	Mod- erate	
56	8.5	-----	7	.45	>20	----	----		-----	---	.04	.02 - .05	No	High	Mod- erate	Mod- erate	Slight
41	4.4	-----	24	.35	8	.7	6,050			1.5	.07	.01 - .03	No	Slight	Slight around wire	Slight	Slight
87	3.1	-----	20	.3	5	2.8	11,300			2.8	.09	.03 - .17	No	None	High around wire	Slight	Slight
850c	3.1	-----	18	.4	5	1.9	8,060		-----	2.0	.06	.02 - .20	No	None	Mod- erate around wire	Mod- erate	Slight





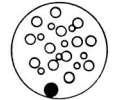


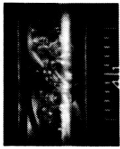

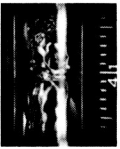
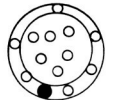
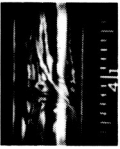
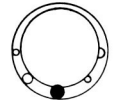

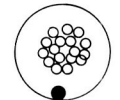


(b) Vertically upward flow at 1 g

33	8.5	-----	12	0.50	20	0.08	6,050			1.5	0.06	0.03 - 0.08	No	Slight	Slight around wire	None
34	8.5	-----	31	.50	12	1.4	14,930		-----	3.7	.09	.02 - .30	Pos- sibly	Slight	Mod- erate around big bubbles	Mod- erate around big bubbles
57	8.5	-----	60	.50	14	---	---		-----	---	.05	.02 - .08	No	Slight	Very slight	Very slight
859	3.1	-----	1	.40	8	---	---			---	.02	None	No	None	No bubbles	Slight

(c) Vertically downward flow at 1 g

ass	3.1	-----	1/2	0.3	6	-----	-----	-----	---	0.02	None	No	None	No bubbles	None
															

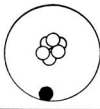

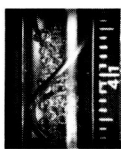
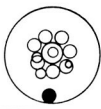

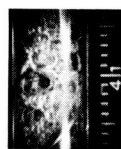
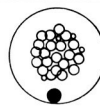
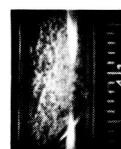
(d) Flow at 0 g

lc	8.5	Free floating	27	0.45	10	0.1	3,630			0.9	0.2	0.1 - 0.3	Yes	None	None	Slight around coalescence
ld	8.5	Free floating	27	.45	10	.1	4,030		Same as run lc	1.0	.2	.1 - .3	Yes	None	None	Slight around coalescence
44	8.5	Restrained	2	.45	20	.09	6,460			1.6	.04	.02 - .06	No	Slight	Slight	Slight
46	8.5	Restrained	12	.50	14	.2	6,860			1.7	.06	.02 - .11	No	Moderate	Slight	Slight
30	4.4	Free floating	12	.30	12	.1	6,050			1.5	.20	.05 - .40	Yes	None	None	Moderate around coalescence
a31	4.4	Free floating	55	.40	8	1.2	10,100			2.5	.10 and slugs 0.40 by 0.50 in. long	.05 - .40	Yes	Slight	Moderate	High
32	4.4	Restrained	65	.40	None	0	7,270			1.8	.10 and slugs 0.40 by 2 in. long	.05 - .40	Yes	High	Moderate	Moderate
41	4.4	Restrained	10	.35	8	.4	6,050			1.5	.05	.01 - .07	No	None	Slight around wire	Slight
42	4.4	Restrained	70	.45	8	1.1	9,300			2.3	.10	.02 - .45	Pos- sibly	None	None	None

*Included in film supplement.


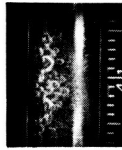
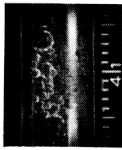

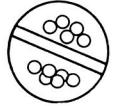
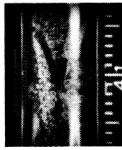

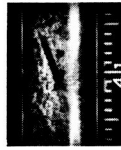
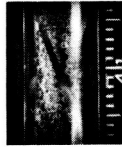
TABLE II. - Concluded. SWIRLING TWO-PHASE FLOW WITH COILED-WIRE SWIRL GENERATORS

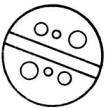
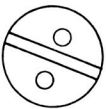


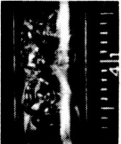
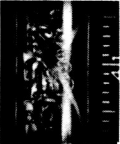
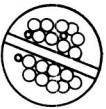
(d) Concluded. Flow at 0 g

Run	Insert diameters- per-coil ratio	Experi- mental technique	Approximate air volume, percent	Approximate core diameter, in.	Approximate core rotation, diam/rev- olution	Induced radial acceleration, g	Reynolds number	Flow model		Bubble						
								Full-scale cross section	Reduced side view (Flow →)	Average velocity, ft/sec	Diameter, in.		Coales- cence	Velocity gradient	Turbulence	
											Range	Average			Wall	Free stream
a8	3.1	Restrained	7	0.20	3	1.5	6,460			1.6	0.10	0.10 - 0.15	No	None	None	Slight
a11	3.1	Free floating	7	.20	3.4	1.5	6,860	Same as run 8		1.7	.10	.10 - .15	No	None	None	Slight
14	3.1	Restrained	23	.30	4	4.0	10,900		-----	2.7	.10	.07 - .15	No	None	None	Slight
a50a	3.1	Restrained	80	.50	5	.9	4,850			1.2	.10	.02 - .35	Pos- sibly	None	None	Slight
a50b	3.1	Restrained	12	.35	5	.5	4,440			1.1	.06	.02 - .08	No	None	None	Slight

^aIncluded in film supplement.

TABLE III. - SWIRLING TWO-PHASE FLOW AT O G WITH TWISTED-RIBBON SWIRL GENERATORS

Run	Insert diameters- per-twist ratio	Experi- mental technique	Approximate air volume, percent	Reynolds number	Flow model		Bubble						
					Full-scale cross section	Reduced side view (Flow →)	Average velocity, ft/sec	Diameter, in.		Coa- les- sence	Velocity gradient	Turbulence	
								Average	Range			Wall	Free stream
a21	7.5	Free floating	36	7740			2.4	0.08	0.04 - 0.22	Pos- sibly	None	None	None
a22	7.5	Restrained	36	8060	Same as run 21		2.5	.08	.04 - .22	Pos- sibly	None	None	None
23	7.5	Restrained	26	3880		-----	1.2	.08	.04 - .09	None	Slight	None	None
16	4.2	Restrained	20	4200			1.3	.09	None	None	None	None	None
17	4.2	Restrained	35	8060			2.5	.09	.07 - .20	Yes	None	None	None ^b
18	4.2	Free floating	20	5170	Same as run 16		1.6	.09	None	None	None	None	None
19	4.2	Free floating	35	9680	Same as run 17	-----	3.0	.09	.07 - .20	Yes	None	None	None ^b

24	2.7	Restrained	2	2590		-----	0.8	0.10	0.02 - 0.15	Yes	None	None	Slight
a25	2.7	Restrained	1	4840			1.5	.10	.02 - .15	Yes	None	None	Slight
a26	2.7	Restrained	25	6140			1.9	.20 and slugs 0.30 in. long	None	Yes	None	None	Moderate
a27	2.7	Free floating	25	6780	Same as run 26		2.1	.20 and slugs 0.30 in. long	None	Yes	None	None	Moderate
a51	2.7	Restrained	19	4520		-----	1.4	.07	.02 - .13	None	None	None	None

^aIncluded in film supplement.

^bSome turbulence around coalescing bubbles.

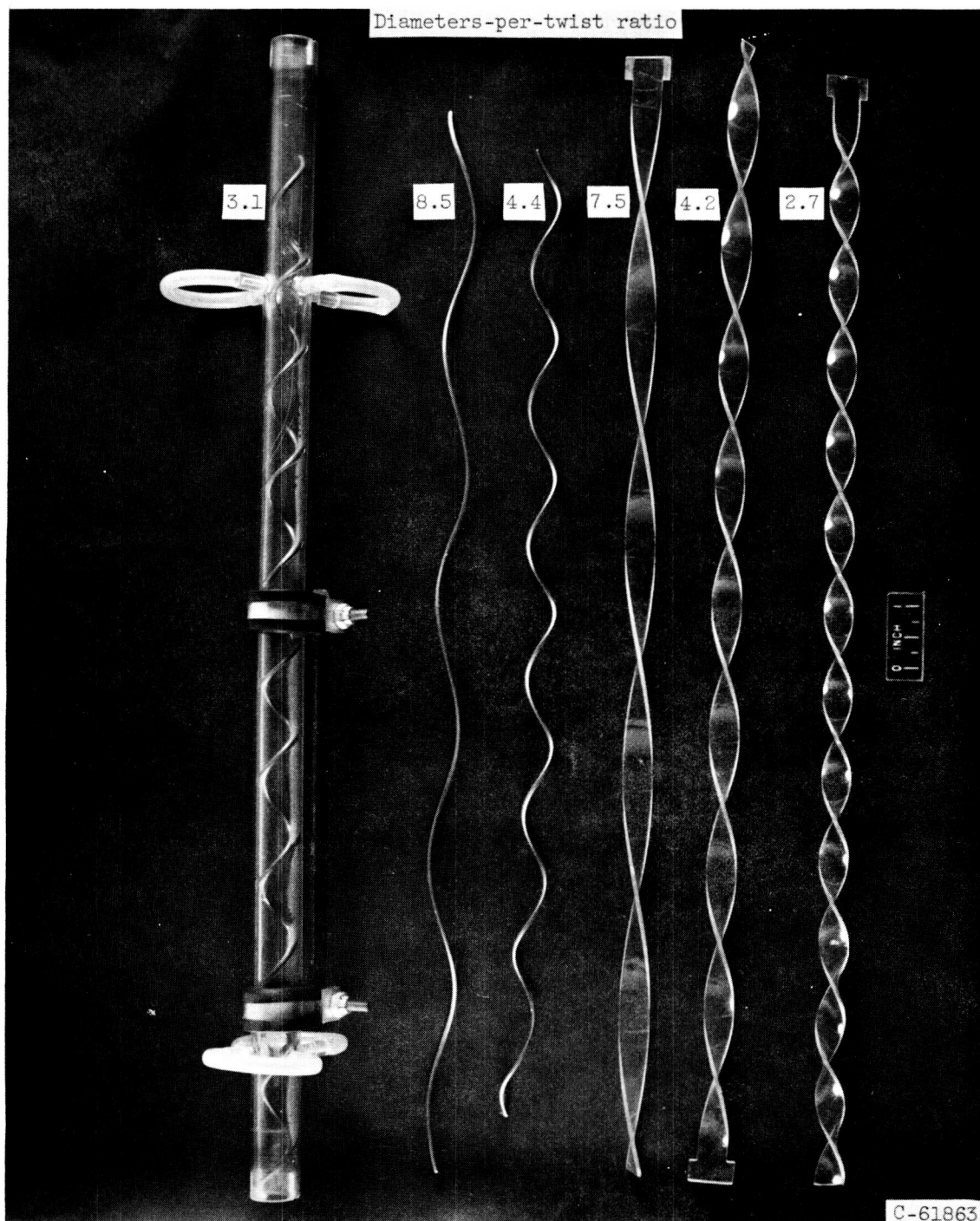
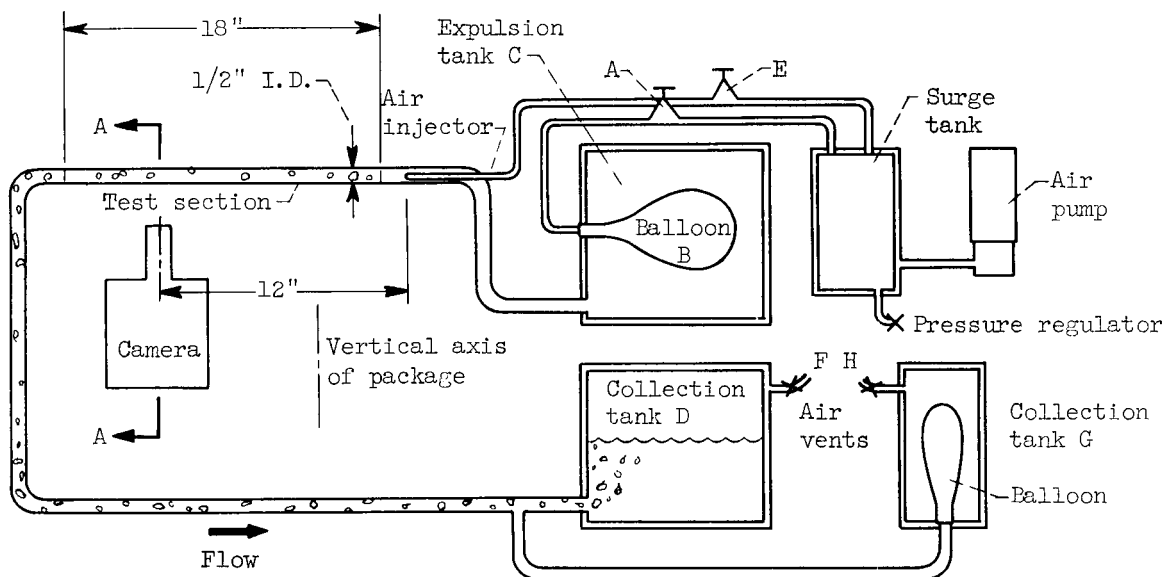
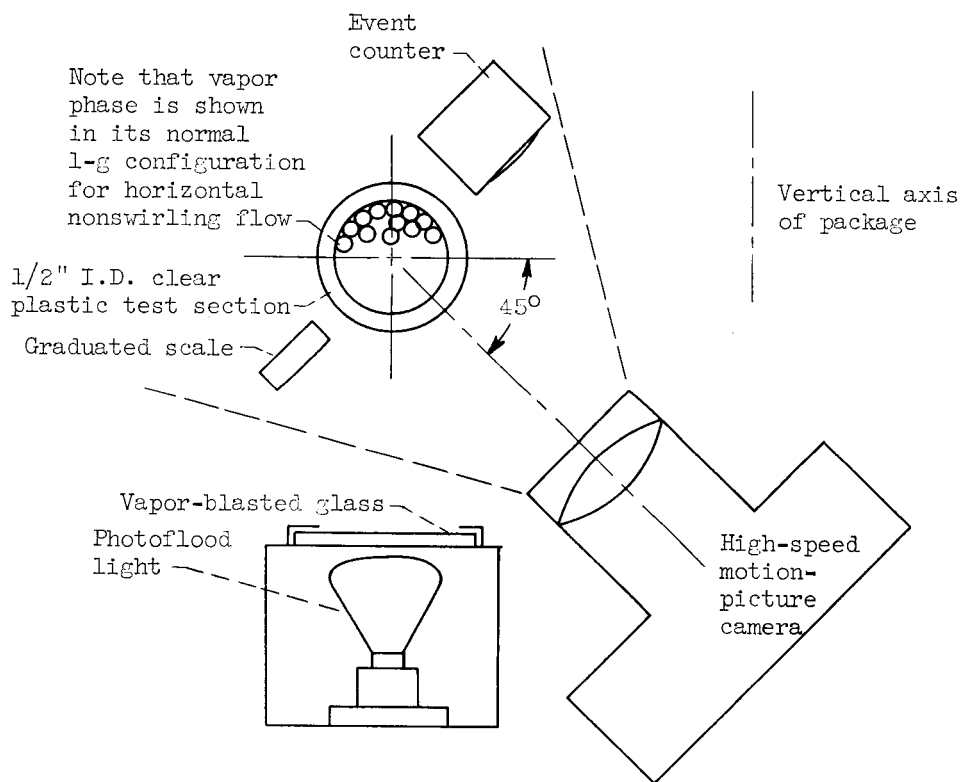


Figure 1. - Clear-plastic test section and coiled-wire and twisted-ribbon swirl generators.

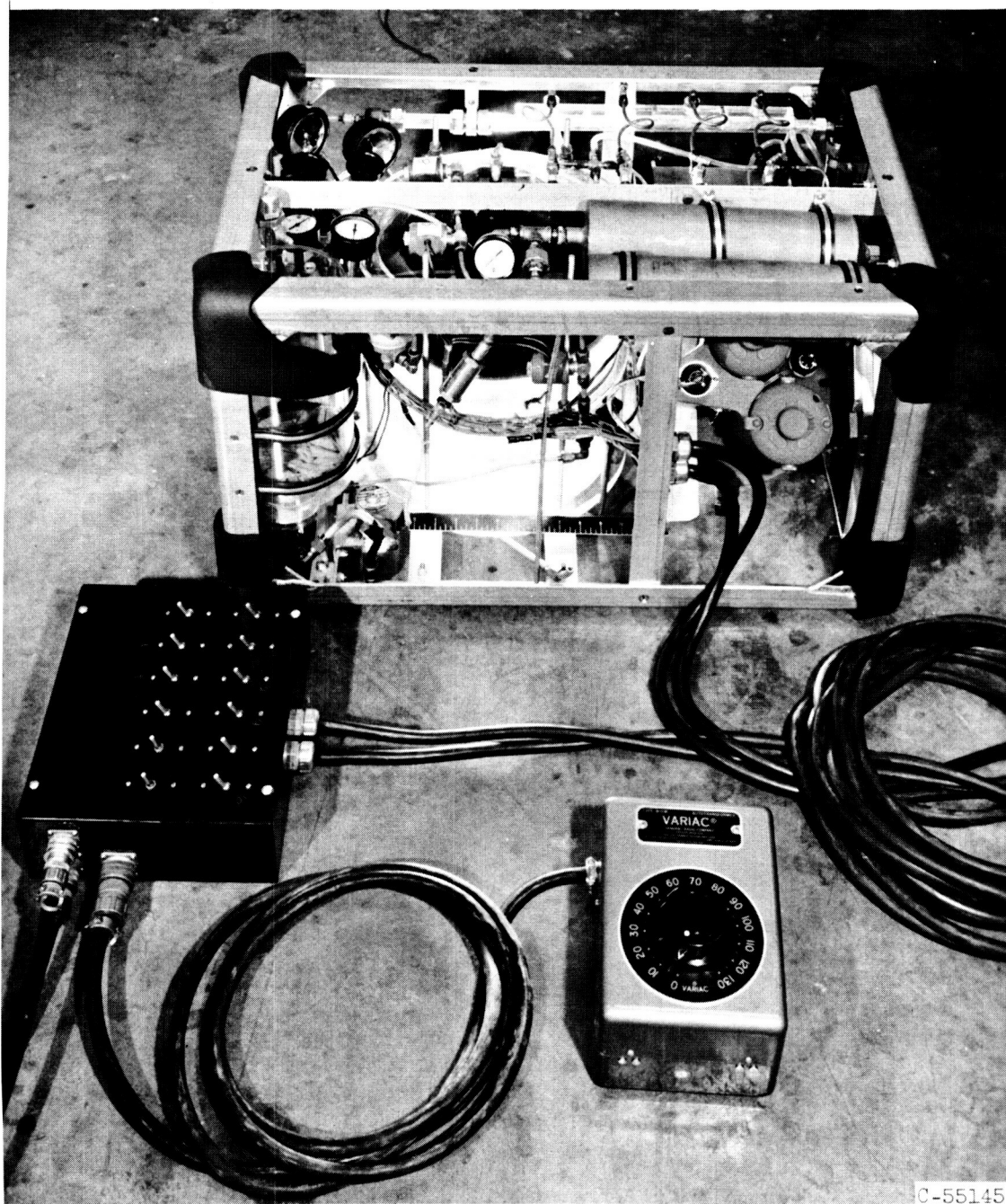


(a) Flow diagram.



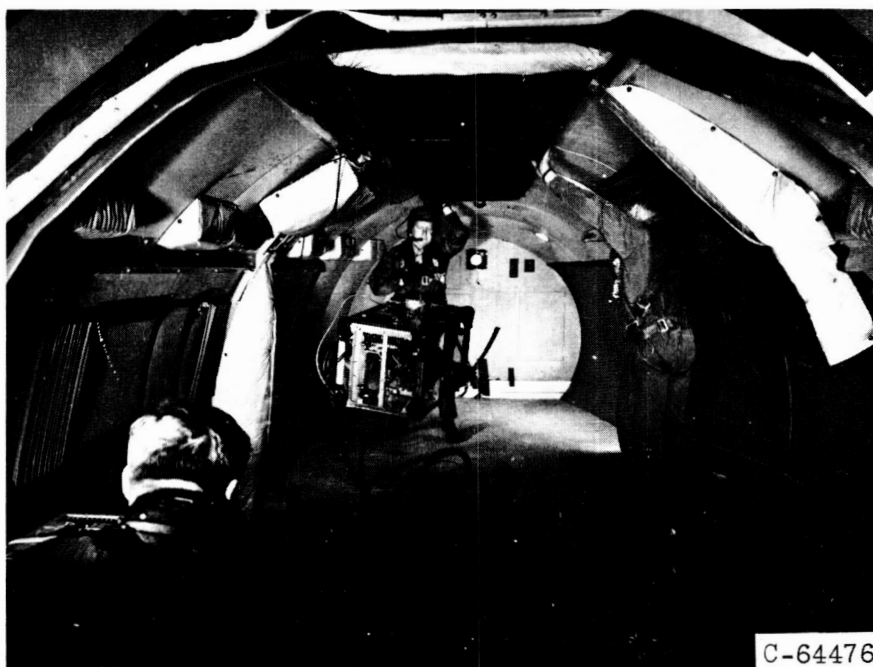
(b) Section A-A: Schematic diagram of relation between camera, test section, and light box.

Figure 2. - Experimental apparatus.



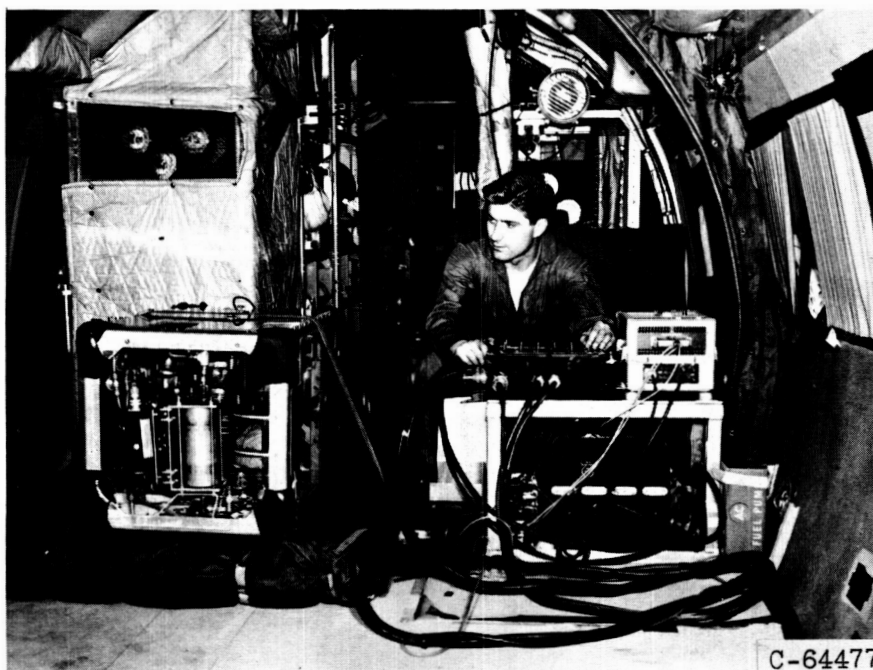
C-55145

Figure 3. - Experimental package, control box, and camera transformer.



C-64476

(a) Free-floating experimental package.



C-64477

(b) Restrained experimental package.

Figure 4. - Experimental equipment installed in C-131b aircraft.



C-64478

(a) C-131b.



C-59877

(b) AJ-2.

Figure 5. - Zero-g aircraft facilities.

	Event	Acceler- ation, g	Time, sec
A	Dive	1	25
B	Pullup	2 - 3	5
C	Weightlessness	0	10 - 15
^a D	Pullup	1	4
E	Pullup	2 - 3	4 - 6

^aIncluded only in run 50.

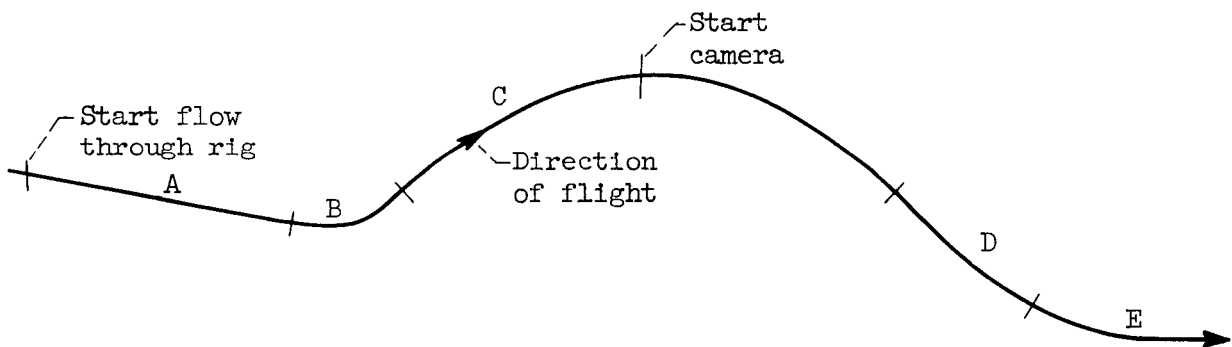


Figure 6. - Schematic drawing of 0-g flight maneuver.